

A. Nid, S. Sayah, A. Zebar

Power fluctuation suppression for grid connected permanent magnet synchronous generator type wind power generation system

Introduction. Weather changes lead to create oscillations in values of power extracted from renewable energy resources (RERs). These power oscillations pose significant challenges in RERs integration process with the power grid systems, through its effects on power system stability. Many studies have been performed in various methods to mitigate the output power fluctuation of wind power generation system (WPGS). **Purpose.** This study focuses on increasing the mitigation rate of the output power fluctuation of WPGS caused by the rapid wind speed changes during wind gusts. Superconducting magnetic energy storage (SMES) system through its properties represents an effective solution for the WPGS power fluctuation issue. WPGS and SMES systems are linked to power grid system through the point of common coupling (PCC). **Methods.** This paper proposes two robust controllers for controlling the SMES system. The first controller is a Fuzzy Logic Controller (FLC), which has been utilized for controlling the power exchange between the SMES coil and the PCC of the utility grid. While the second controller is a PI controller, which have been utilized to regulate the voltages between the two sides of the PCC and the DC link capacitor in the SMES system. The proposed controllers have been constructed so that can make the SMES system absorb/deliver the real power instantaneously from/toward PCC according the wind speed changes. MATLAB/Simulink has been utilized to simulate the system under study and test the performance of proposed controllers. In addition, two different wind speed scenarios have been used in the simulation. **Practical value.** Results of simulation have proven the effectiveness of proposed controllers so that the active power fluctuation delivered to utility grid can be reduced by up to 89 %. References 31, tables 4, figures 9.

Key words: wind power generation system, power grid system, superconducting magnetic energy storage, fuzzy logic control.

Вступ. Зміни погоди призводять до коливань значень потужності, що надходять з відновлюваних джерел енергії (RERs). Ці коливання потужності створюють серйозні проблеми у процесі інтеграції RERs з енергосистемами через їх вплив на стабільність енергосистеми. Було проведено велику кількість досліджень різних методів пом'якшення коливань вихідної потужності системи вітрогенерації (WPGS). **Мета.** Це дослідження спрямоване на підвищення ступеня пом'якшення коливань вихідної потужності WPGS, викликаних швидкими змінами швидкості вітру під час поривів вітру. Система надпровідного накопичення магнітної енергії (SMES) завдяки своїм властивостям є ефективним вирішенням проблеми коливань потужності WPGS. Системи WPGS та SMES пов'язані з енергосистемою через точку загального підключення (PCC). **Методи.** У цій статті пропонуються два робастні контролери для управління системою SMES. Перший контролер є контролером нечіткої логіки (FLC), який використовувався для управління обміном енергії між котушкою SMES і PCC енергосистеми. У той час як другий контролер є ПІ-регулятором, який використовувався для регулювання напруг між двома сторонами PCC і конденсатором кола постійного струму в системі SMES. Пропоновані контролери були сконструйовані таким чином, щоб система SMES могла миттєво поглинати/передавати реальну потужність від/до PCC відповідно до змін швидкості вітру. MATLAB/Simulink використовувався для моделювання досліджуваної системи та перевірки продуктивності пропонованих контролерів. Крім того, при моделюванні використовувалися два різні сценарії швидкості вітру. **Практична цінність.** Результати моделювання довели ефективність пропонованих контролерів, що дозволяють знизити до 89 % коливання активної потужності, що подається до енергосистеми. Бібл. 31, табл. 4, рис. 9.

Ключові слова: вітроенергетична система, система електромережі, надпровідний магнітний накопичувач енергії, керування на нечіткій логіці.

Abbreviations

DFIG	Doubly Fed Induction Generator	PWM	Pulse-Width Modulation
ESS	Energy Storage System	RER	Renewable Energy Resource
FLC	Fuzzy Logic Controller	SMES	Superconducting Magnetic Energy Storage
MF	Membership Function	SC	Superconductor
PMSG	Permanent Magnet Synchronous Generator	VSC	Voltage Source Converter
PV	Photovoltaic	WPGS	Wind Power Generation System
PCC	Point Of Common Coupling		

Introduction. Nowadays, with climate changes and the appearance of global warming, RERs have become increasingly used, unlike solar energy [1, 2]. RERs are environmentally friendly because of their low carbon emissions, whereas conventional generation sources with high carbon emissions have serious environmental impacts. The most prevalent RERs are wind, biomass and PV solar [3, 4]. Due to its high efficiency, WPGS has the fastest growth rate among other forms of power generation. However, the major disadvantage of the WPGS is that the amount of generated power depends entirely on the wind speed, so the output power of the WPGS will fluctuate. Therefore, the stability of the power grid system will be influenced. In addition the output power fluctuations of the WPGS can affect directly the power transfer capability, voltage and frequency stability profiles at the power grid system's connection point, knowing that the voltage and

frequency deviation values are of major importance for measuring the level of the power grid stability [5]. In order to ensure a more reliable and economical energy to the customers, ESSs such as flywheels [6], batteries [7, 8], pumped hydro [9, 10], super capacitor [11], etc., are widely used in renewable power generation systems. ESSs are essential elements that have a significant role in solving the mentioned WPGS issues. This can be achieved through the charging and discharging features of the ESS, which ensure a more power balance between RER and loads. Nevertheless, battery and flywheel ESSs have some drawbacks, such as their very slow responses to compensate the power fluctuation as well as short lifetimes and low efficiency [12].

Currently, SMES system is considered one of the most optimal choices for solving the above-mentioned

© A. Nid, S. Sayah, A. Zebar

issues by mitigating the output power fluctuation of the WPGS. SMES systems present many advantages such as high efficiency, long lifetime, short time delay during the charging/discharging processes, lower power losses especially at standby operation, very fast response time, and low maintenance requirements [13].

Several studies related to SMES applications in renewable power generation systems have been reported in the literature. Some of these works have focused on installing SMES systems at PCC to improve the performance of WPGS during voltage sag/swell on the power system side [14]. In [15] a SMES device has proposed to power fluctuation suppression and active filtering in PV microgrid. The application of high temperature superconducting devices in a distribution grid for mitigating issues associated with the large-scale penetration of renewable energy has been studied in [16]. In [17] a new effective technique has developed to improve the performance of DFIG-based WECS during wind gust using a high temperature SC. The performance of a battery/SMES hybrid ESS used in a hybrid power system with fuel cells and RERs under an unknown load profile was discussed in [18]. Authors in [19] have proposed the SMES units controlled by self-tuned algorithm in order to smooth out the output power of wind plants. For a more reliable grid connection of superconducting wind turbine generators, authors in [20] have suggested a cooperative strategy integrated with a SMES device and two modified wind turbine generator controls. On the other hand, a new hybrid PV SMES system controlled by a PID fuzzy controller has been studied in [21] in order to minimize the oscillation of the PV extracted power.

The goal of the paper is increasing the mitigation rate of the output power fluctuation of WPGS caused by the rapid wind speed changes during wind gusts.

This paper proposes two robust controllers for SMES systems in order to smooth out the power provided by a WPGS based on PMSG integrated with utility grid. The first controller is a FLC which operates with a DC-DC chopper circuit for controlling the power exchanged between the SMES coil and the PCC of the utility grid. The second controller is a PI controller whose role is to attempt to keep the voltages between both the PCC sides and DC link capacitor sides of the VSC according to the rated values of the SMES system. This is for giving a flexible and rapid exchange of real power as well as to satisfy requirements of coupling the SMES system with the PCC on the utility grid. The wind speed fluctuations are taken into consideration during the implementation of the proposed controllers. The purpose of these controllers is to make the SMES system capable of absorbing energy from WPGS during situations where wind speed is higher than its rated value, while it is delivering the stored energy in SMES coil during situations where wind speed is lower than its rated value. This strategy can help of smoothing out the power fluctuations of WPGS based on PMSG integrated with the utility grid and make the power steady.

Basic topology and dynamic models. In this work, the wind turbine based on PMSG is used as WPGS. The basic topology of the system under study and the SMES system is shown in Fig. 1, which contains of wind turbine,

PMSG, rectifier, boost converter, inverter, two-step up transformers, filter, SMES system (SC coil, DC-DC chopper, VSC, filter) and the utility grid.

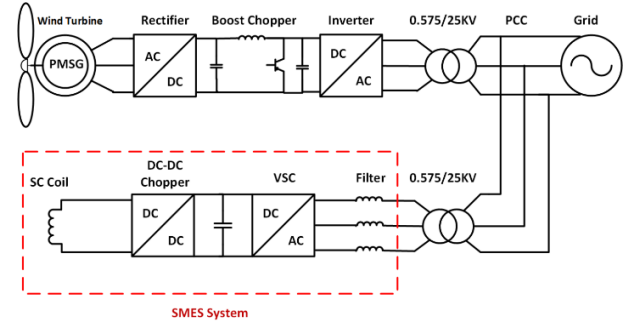


Fig. 1. Basic topology of the system under study and the SMES system

Modeling of wind turbine. The wind turbine is a mechanical machine, which has the ability of transforms the kinetic energy of the wind into mechanical rotational energy that can be exploited by the PMSG. The output power of a wind turbine can be expressed as follows [22]:

$$P_w = \frac{1}{2} \rho \pi R^2 V_w^3 C_p(\lambda, \beta), \quad (1)$$

where P_w is the mechanical power, which is generated by the wind turbine; ρ is the air density; R is the blade radius; V_w is the wind speed; C_p is the power coefficient, which is a function of both tip speed ratio λ and blade pitch angle β .

The tip speed ratio λ of the rotor can be defined as follow [22]:

$$\lambda = V_r R / V_w, \quad (2)$$

where V_r is the rotor speed.

The power coefficient C_p is given by [22]:

$$C_p(\lambda, \beta) = 0.73 \left(\frac{151}{\lambda_i} - 0.58\beta - 0.002\beta^{2.14} - 13.2 \right) \cdot e^{-\frac{18.4}{\lambda_i}}, \quad (3)$$

where λ_i is calculated as [22]:

$$\lambda_i = \frac{1}{\frac{1}{\lambda + 0.02\beta} - \frac{0.003}{\beta^3 + 1}}. \quad (4)$$

Modeling of PMSG. PMSG transforms the mechanical rotational energy to electrical energy that can be exploited for supplying the loads. Table 1 shows the used PMSG parameters in this work. The voltage of stator along the direct and quadrature ($d-q$) axes are written as follows [23]:

$$v_{ds} = R_s i_{ds} + L_d \frac{di_{ds}}{dt} - \omega_e L_q i_{qs}; \quad (5)$$

$$v_{qs} = R_s i_{qs} + L_q \frac{di_{qs}}{dt} + \omega_e \lambda_m + \omega_e L_d i_{ds}; \quad (6)$$

$$\omega_e = p \omega_r. \quad (7)$$

The mechanical dynamic equations of the PMSG can be written as follows [23]:

$$J \frac{d\omega_r}{dt} + D \omega_r = T_m - T_e; \quad (8)$$

where the electromagnetic torque developed can be given by [23]:

$$T_e = \frac{3}{2} p \cdot \left[(L_d - L_q) \cdot i_{ds} i_{qs} - \lambda_m i_{qs} \right]. \quad (9)$$

Table 2

Parameters of the proposed SMES system

Parameter	Value
Chopper switching frequency, kHz	2
VSC switching frequency, kHz	4
SMES inductance, H	0.5
Filter inductance, mH	0.41
DC link capacitor, mF	15
DC link voltage, kV	1
SMES energy, MJ	0.422
SMES current, kA	1.3

The charged and discharged energy in [J] and the active power in [W], exchanged by the SC coil can be calculated as follows [25]:

$$E_{sc} = \frac{1}{2} \cdot L_{sc} I_{sc}^2; \quad (12)$$

$$P_{sc} = \left(L_{sc} \frac{dI_{sc}}{dt} \right) I_{sc} = V_{sc} I_{sc}, \quad (13)$$

where L_{sc} is the self-inductance of SC coil; I_{sc} , V_{sc} are the operating current and voltage of SC coil, respectively.

As shown in Fig. 2, the charge and discharge process of the SC coil is controlled by converting the duty cycle value D given by the FLC into pulse signals generated with the PWM block. These pulse signals feed directly to the IGBT switches gates of the DC-DC chopper. So that if the duty cycle is larger than 0.5, the SC coil is in charge mode, while if the duty cycle is less than 0.5 the SC coil is in discharge operation, and it is still in standby mode if the duty cycle is equal to 0.5. The relation between the voltage across the SC coil V_{sc} and the DC-link voltage V_{dc} can be expressed as follows [25]:

$$V_{sc} = (1 - 2D) \cdot V_{dc}; \quad (14)$$

$$I_{dc} = (1 - 2D) \cdot I_{sc}; \quad (15)$$

where I_{dc} is the DC current flowing between a two quadrant DC-DC chopper and VSC; I_{sc} is the DC current of the SC coil.

Bidirectional VSC. Figure 2 shows the connection of VSC circuit in SMES system. VSC is a high-power self-commutated converter, which can be established using 6 IGBT switches. In the VSC, the AC side is linked with a DC side with the ability to transmit power in both sides. Moreover, VSC can operate at a very high-frequency range (2–20 kHz), allowing it to control both real and reactive power whether independently or simultaneously. The DC-link voltage can be maintained at almost steady level of its reference value by the installed DC-link capacitor, that's in order to make the SMES system more effective in the real power exchange with the PCC.

The proposed SMES system controllers. In this paper, two controllers is used to controls the SMES system. The first is an FLC controller, which is designed to control the used type-D chopper, while the second is a PI controller for the VSC converter. The two controllers are represented in Fig. 2.

DC-DC chopper control operation. FLC is a progressing control technique used in several physical systems such as the electrical distribution systems. FLC is cheaper to develop, fast, does not need a mathematical model, robust and simple to use [26–28]. As represented in Fig. 2, the FLC comprises two inputs, as well as an output. The first input is the PMSG output power, while

The real and reactive power, respectively, are given in d - q frame by the following equations [24]:

$$P_{pmsg} = \frac{3}{2} \cdot [v_{sd} i_{sd} + v_{sq} i_{sq}]; \quad (10)$$

$$Q_{pmsg} = \frac{3}{2} \cdot [v_{sq} i_{sd} - v_{sd} i_{sq}], \quad (11)$$

where λ_m is the magnetic flux of the PMSG; ω_e is the electrical angular speed of PMSG; ω_r is the rotational rotor speed of the turbine's shaft; i_{sd} , i_{sq} are the d - and q - axis stator currents of PMSG; J is the moment of inertia of PMSG; L_s is the synchronous inductance of the PMSG; p is the pole pair number of the PMSG; P_{pmsg} , Q_{pmsg} are the real and reactive powers of PMSG; R_s is the stator resistance of PMSG; T_m , T_e are the mechanical and electromagnetic torque of PMSG; v_{ds} , v_{qs} are the d - and q -axis stator voltages of PMSG.

Parameters of the PMSG

Parameter	Value
Nominal power, MW	1.5
Nominal stator voltage, V	575
Nominal frequency, Hz	50
Number of pole pairs	48
Generator inductance in the d frame, p.u	0.85
Generator inductance in the q frame, p.u	0.85
Generator stator resistance, p.u	0.0012
Flux of the permanent magnets, p.u	0.65

Table 1

SMES system and proposed controllers.

SMES system. As depicted in Fig. 2, the proposed SMES system contains a coupling transformer, a filter, bidirectional VSC-based IGBT switches, a DC link capacitor, a DC-DC chopper-based IGBT switches and SC coil. To adapt and achieve an optimal power exchange between both of power grid and SMES coil sides, power electronic converters (bidirectional VSC, DC-DC chopper) must be linked between them. SMES system parameters are chosen in such a way that they can effectively address the power fluctuations of the WPGS-based PMSG. Table 2 shows the proposed SMES system parameters.

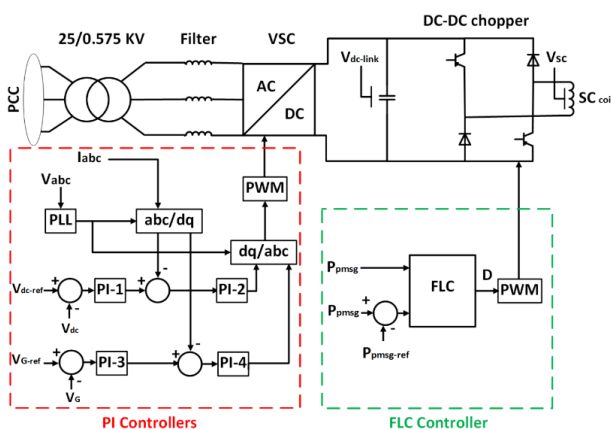


Fig. 2. The structure of the proposed SMES system with its controllers

Type-D chopper shown in Fig. 2 is a type of DC-DC converter that can controls the charge and discharge process of the SC coil. It works by rapidly switching the IGBTs on and off, which in turn controls the amount of exchanged energy between the SC coil and PCC.

the second input is taken from the result of subtraction between the output of PMSG and its reference value. The duty cycle is taken as an FLC output. MFs of the FLC are depicted in Fig. 3. The triangular MFs type has been used in both fuzzification and defuzzification processes.

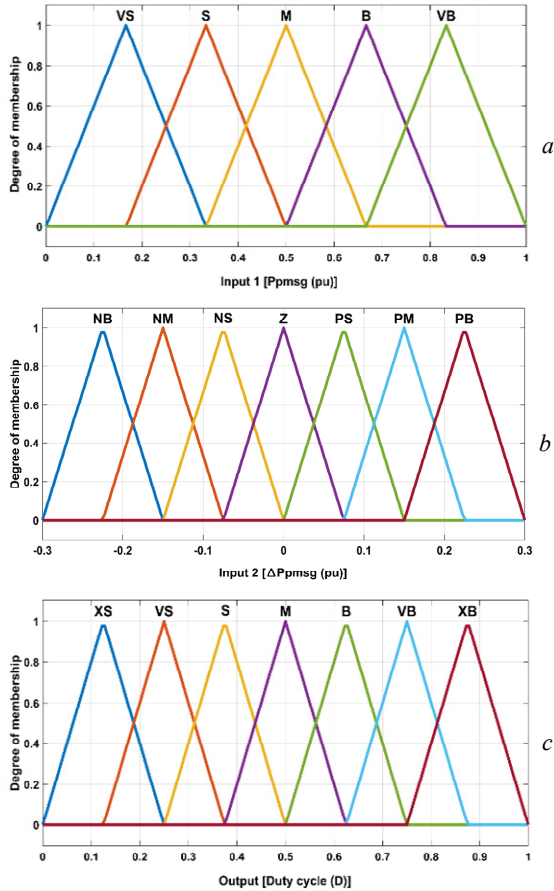


Fig. 3. MFs of inputs/output variables of FLC: a – input № 1; b – input № 2; c – output

The triangular MFs can be evaluated as a function of vector x as follows [29]:

$$f(x, a, b, c) = \max\left(\min\left(\frac{x-a}{b-a}, \frac{c-x}{c-a}\right), 0\right), \quad (16)$$

with $a \leq b \leq c$, where a, c are the coordinates locations of feet of the triangle; b is the coordinate location of the peak; x is the value of the input or output variable.

The fuzzy inference system uses the Mamdani method to build the FLC rules. This strategy depends on IF/ THEN rule to construct the decision table for determining the FLC output values. The FLC output defuzzification process has been achieved using the center of gravity method.

The duty cycle values, which have been considered as the output of FLC in this study, can be evaluated according to the surface graph of Fig. 4.

VSC control operation. As shown in Fig. 3, the VSC control is performed using PI controllers in order to maintain the voltages of AC and DC sides in specified ranges according to predetermined values. The power flow direction between AC and DC sides is determined based on the actual voltages on the two sides of VSC. A phase-locked loop has been employed in PI controllers for coupling the SMES system with both the WPGS system

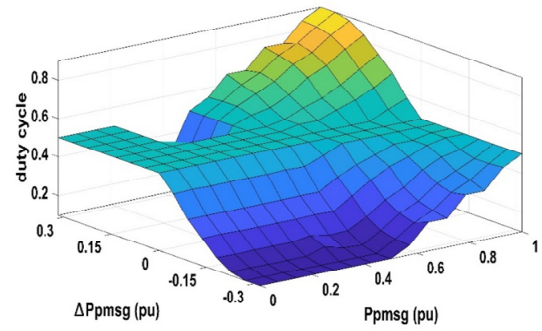


Fig. 4. Surface graph of FLC output variable

and the power grid, so that it has been used in the VSC voltages synchronization process with grid voltages. The reference currents of $d-q$ axis can be taken from the subtraction result values of both DC link reference voltage/DC link actual voltage and AC reference voltage/AC actual voltage, respectively. The PI controllers convert the comparison results between the reference currents of $d-q$ axis and their actual values obtained by the abc/dq block into controlled voltage signals in $d-q$ axis. These voltage signals can be converted to three-phase sinusoidal signals by dq/abc block. These sinusoidal signals are taken as reference voltages, which are utilized by the PWM block to produce PWM pulse signals to feed IGBT switch initiation processes in the VSC converter. The gains of the PI controllers are given in Table 3.

Table 3

Parameters of the PI controller				
Gains	PI-1	PI-2	PI-3	PI-4
K_p	0.32	0.018	0.16	0.05
K_i	8	247	725	183

Simulation results and discussions. In this part, the proposed controllers for the SMES system were implemented using the MATLAB/Simulink software. As shown in Fig. 5, two wind speed scenarios were used in order to simulate the fluctuations of the power generated by WPGS. In order to verify the effectiveness of the proposed SMES system, significant and sudden changes were chosen for each scenario of wind speed.

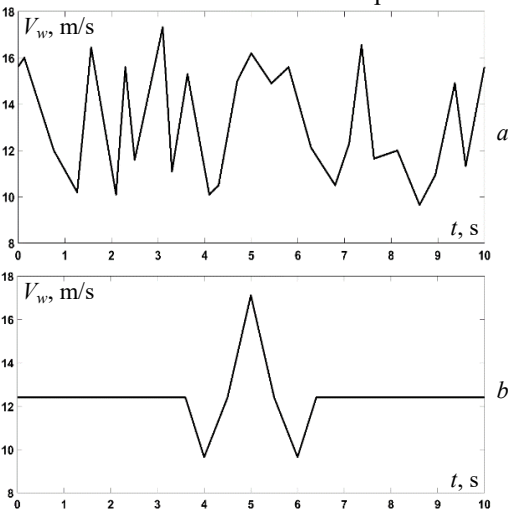


Fig. 5. Wind speed scenarios: a – scenario № 1; b – scenario № 2

For comparison purposes, simulations were firstly performed without considering SMES system and then by including the proposed SMES system. The rated power

value was taken at a $V_w = 12.3$ m/s, which is considered as the rated speed of wind turbine. Simulation results for duration of 10 s including the active power at PCC and SMES active power are illustrated in Fig. 6, 7, respectively. It is clearly from the first scenario (Fig. 6,*a*) that the real power at the PCC fluctuates between the two limits: 1.31 p.u. and 0.49 p.u. when the SMES system is not installed, while it fluctuates between 1.05 p.u. and 0.96 p.u. limits when the SMES system is installed. Consequently, for scenario №1 the real power fluctuation at PCC is reduced by 89.02 %.

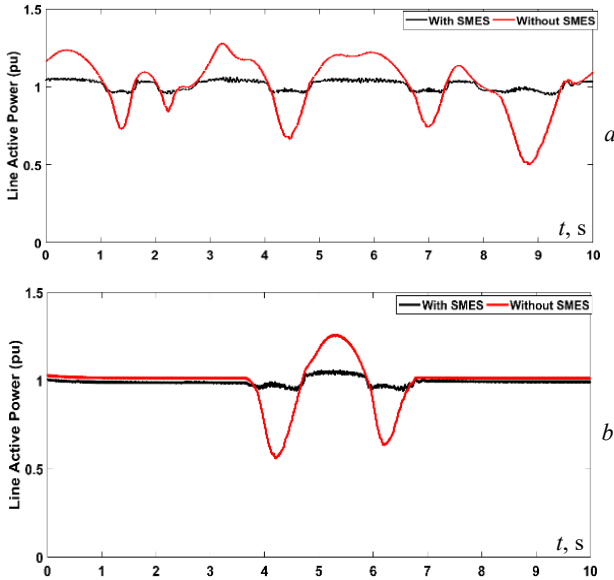


Fig. 6. Response of the active power at PCC during wind gusts: *a* – scenario № 1; *b* – scenario № 2

Likewise, for the second scenario (Fig. 6,*b*) the real power at PCC fluctuates between 1.27 p.u. and 0.56 p.u. limits when the SMES system is not installed, while it fluctuates between the limits 1.05 p.u. and 0.96 p.u. when the SMES system is installed, giving a reduction of 87.32 % in the PCC real power fluctuation. As a result, the findings clearly demonstrate that the proposed SMES system has the capability to decrease the fluctuations of WPGS real power delivered to the power grid.

Besides, it can be seen from Fig. 7 that the direction of SMES real power is directly affected by both the change of real power value produced by WPGS and the wind speed. Therefore, if the output real power of WPGS is more than its rated value, the SMES system absorbs the real power excess from the PCC. On the other hand, if the output real power of WPGS is less than its rated value, the SMES system supplies the power deficiency to the PCC. When the WPGS output real power is equal to its rated power, the SMES system is kept at standby mode.

Figure 8 shows the curve of stored energy in the SMES coil as well as the curve of current flowing through the SMES coil for the two scenarios. It is obvious that the stored energy in the SMES coil and the current flow through the SMES coil are directly dependent on the change of power value produced by the WPGS. Moreover, the proposed SMES system can rapidly exchange energy during charging and discharging process; this is a result of the fast response of the proposed FLC technique.

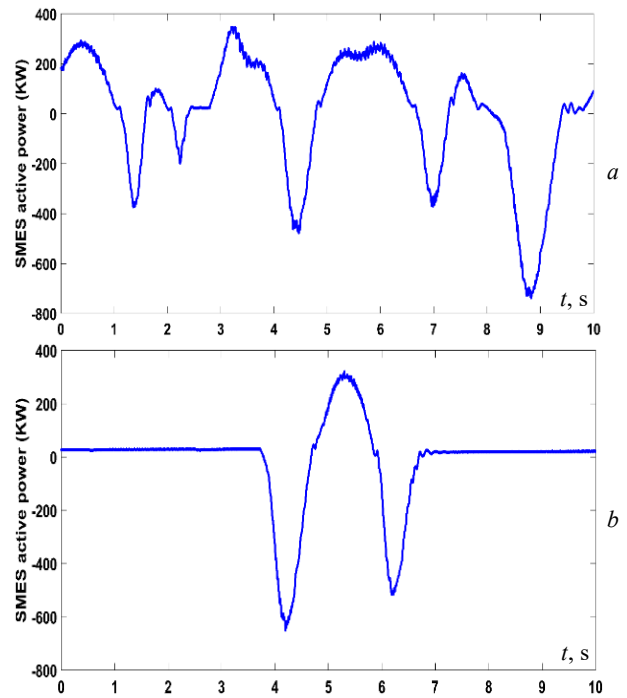


Fig. 7. Response of SMES active power during wind gusts: *a* – scenario № 1; *b* – scenario № 2

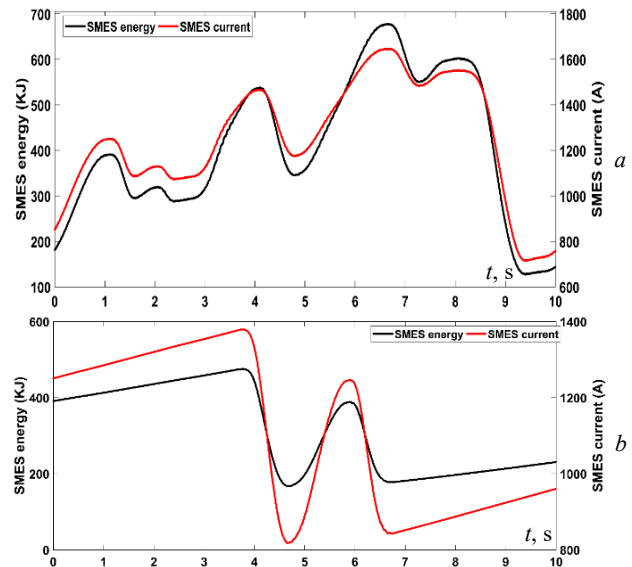


Fig. 8. Behavior of SMES stored energy and current flow through the SMES coil during wind gusts: *a* – scenario № 1; *b* – scenario № 2

Finally, as it can be seen from Fig. 9, the voltage of the SMES DC link capacitor is almost constant and equal to its specified rated value for the two scenarios. This can help in preserving a longer lifetime of the DC link capacitor in the SMES system. These results prove the effectiveness of the proposed PI controllers.

Performance comparison. In order to verify the effectiveness of the proposed SMES system with its controllers, the obtained results of this study are compared with other results reported recently in the literature [30, 31] (Table 4). The comparison includes the SMES capacity used in each study as well as the reduction rate of the real power fluctuations provided by the WPGS. It can be seen from Table 4 that the proposed system gives better reduction rates for the real power

fluctuations than those proposed in the recent literature. It is also clear from Table 4 that the proposed SMES has a lower capacity than that published in the recent studies.

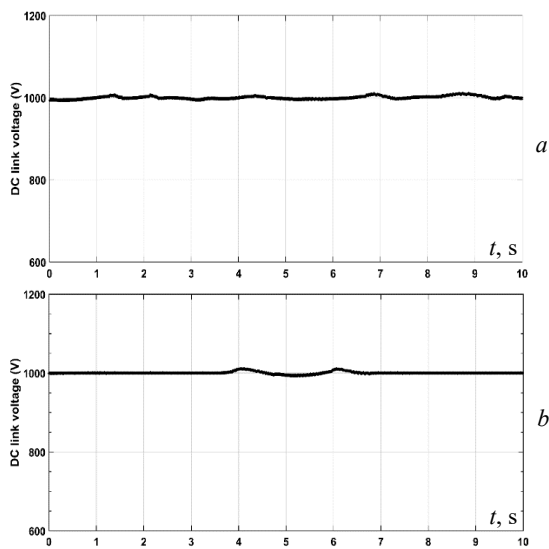


Fig. 9. SMES DC link voltage during wind gusts: a – scenario № 1; b – scenario № 2

Table 4
Comparative study of SMES systems for reduction of power fluctuation generated by WPGS

	9 MW SCIG wind power generation [30]	9 MW DFIG power generation [31]	Proposed: 2 MW PMSG wind power generation
SMES capacity	1 MJ for 2 MW	1.6 MJ for 1.5 MW	0.422 MJ for 1.5 MW
Reduction rate of real power fluctuations for scenario № 1	56.53 %	87.5 %	89.02 %
Reduction rate of real power fluctuations for scenario № 2	53.1 %	71.42 %	87.32 %

Conclusions. In this paper, an effective SMES system with its controllers are proposed to mitigate the fluctuations of power provided by the WPGS based on PMSG integrated with the power grid. The FLC is proposed for controlling the DC-DC chopper circuit, whereas the PI controllers are proposed for controlling the bidirectional VSC circuit. The FLC is designed so that the SMES system can absorb/supply the real power from/to the PCC according to the amount-generated power from the WPGS during wind speed changes. The PI controllers are designed for regulating the voltages on the two sides (PCC and DC link capacitor) of the bidirectional VSC at allowable and predetermined ranges. Simulations were carried out using two different wind speed scenarios. As a result, the following conclusions are drawn:

1. The effectiveness of the proposed PI controllers has proven through the nearly constant at its predetermined value, and avoiding the deep ripples in DC link voltage during the fast charge and discharge processes of SMES coil, consequently this is can help in preserving a longer lifetime of the DC link capacitor.

2. The effectiveness of the proposed FLC has proven by the fast response of the SMES system for

absorbing/supplying the real power from/to the PCC during the wind speed changes.

3. The proposed SMES control strategy is found to be very effective in mitigating the real power fluctuations supplied by the WPGS, where the real power fluctuations were significantly reduced by 89.02 % for the first scenario and 87.32 % for the second scenario.

These results contribute to the improvement of the reliability of the WPGS based PMSG.

Conflict of interest. The authors declare that they have no conflict of interest.

REFERENCES

- Louarem S., Kebbab F.Z., Salhi H., Nouri H. A comparative study of maximum power point tracking techniques for a photovoltaic grid-connected system. *Electrical Engineering & Electromechanics*, 2022, no. 4, pp. 27-33. doi: <https://doi.org/10.20998/2074-272X.2022.4.04>.
- Manikandan K., Sasikumar S., Arulraj R. A novelty approach to solve an economic dispatch problem for a renewable integrated micro-grid using optimization techniques. *Electrical Engineering & Electromechanics*, 2023, no. 4, pp. 83-89. doi: <https://doi.org/10.20998/2074-272X.2023.4.12>.
- Maradin D. Advantages and disadvantages of renewable energy sources utilization. *International Journal of Energy Economics and Policy*, 2021, vol. 11, no. 3, pp. 176-183. doi: <https://doi.org/10.32479/ijeep.11027>.
- Youcef D., Khatir K., Yassine B. Design of neural network fractional-order backstepping controller for MPPT of PV systems using fractional-order boost converter. *International Transactions on Electrical Energy Systems*, 2021, vol. 31, no. 12, art. no. e13188. doi: <https://doi.org/10.1002/2050-7038.13188>.
- Said S.M., Salama H.S., Hartmann B., Vokony I. A robust SMES controller strategy for mitigating power and voltage fluctuations of grid-connected hybrid PV–wind generation systems. *Electrical Engineering*, 2019, vol. 101, no. 3, pp. 1019-1032. doi: <https://doi.org/10.1007/s00202-019-00848-z>.
- Ghanaatian M., Lotfifard S. Control of Flywheel Energy Storage Systems in the Presence of Uncertainties. *IEEE Transactions on Sustainable Energy*, 2019, vol. 10, no. 1, pp. 36-45. doi: <https://doi.org/10.1109/TSTE.2018.2822281>.
- Nayak C.K., Nayak M.R. Technoeconomic analysis of a grid-connected PV and battery energy storage system considering time of use pricing. *Turkish Journal of Electrical Engineering and Computer Sciences*, 2018, vol. 26, no. 1, pp. 318-329. doi: <https://doi.org/10.3906/elk-1703-35>.
- Ali Moussa M., Derrouazin A., Latroch M., Aillerie M. A hybrid renewable energy production system using a smart controller based on fuzzy logic. *Electrical Engineering & Electromechanics*, 2022, no. 3, pp. 46-50. doi: <https://doi.org/10.20998/2074-272X.2022.3.07>.
- Fan J., Xie H., Chen J., Jiang D., Li C., Ngaha Tiedeu W., Ambre J. Preliminary feasibility analysis of a hybrid pumped-hydro energy storage system using abandoned coal mine goafs. *Applied Energy*, 2020, vol. 258, art. no. 114007. doi: <https://doi.org/10.1016/j.apenergy.2019.114007>.
- Bruninx K., Dvorkin Y., Delarue E., Pandzic H., Dhaeseleer W., Kirschen D.S. Coupling Pumped Hydro Energy Storage With Unit Commitment. *IEEE Transactions on Sustainable Energy*, 2016, vol. 7, no. 2, pp. 786-796. doi: <https://doi.org/10.1109/TSTE.2015.2498555>.
- Wujong Lee, Hanju Cha. A supercapacitor remaining energy control method for smoothing a fluctuating renewable energy power. *2013 IEEE ECCE Asia Downunder*, 2013, pp. 398-403. doi: <https://doi.org/10.1109/ECCE-Asia.2013.6579127>.
- Aly M.M., Mohamed E.A., Salama H.S., Said S.M., Abdel-Akher M., Qudaih Y. A Developed Voltage Control Strategy for Unbalanced Distribution System During Wind Speed Gusts Using

- SMES. *Energy Procedia*, 2016, vol. 100, pp. 271-279. doi: <https://doi.org/10.1016/j.egypro.2016.10.177>.
13. Yao C., Ma Y. Superconducting materials: Challenges and opportunities for large-scale applications. *IScience*, 2021, vol. 24, no. 6, art. no. 102541. doi: <https://doi.org/10.1016/j.isci.2021.102541>.
14. Seung-Tak Kim, Byung-Kwan Kang, Sun-Ho Bae, Jung-Wook Park. Application of SMES and Grid Code Compliance to Wind/Photovoltaic Generation System. *IEEE Transactions on Applied Superconductivity*, 2013, vol. 23, no. 3, art. no. 5000804. doi: <https://doi.org/10.1109/TASC.2012.2232962>.
15. Jin J.X., Wang J., Yang R.H., Zhang T.L., Mu S., Fan Y.J., Xing Y.Q. A superconducting magnetic energy storage with dual functions of active filtering and power fluctuation suppression for photovoltaic microgrid. *Journal of Energy Storage*, 2021, vol. 38, art. no. 102508. doi: <https://doi.org/10.1016/j.est.2021.102508>.
16. Rahman O., Muttaqi K.M., Sutanto D. High Temperature Superconducting Devices and Renewable Energy Resources in Future Power Grids: A Case Study. *IEEE Transactions on Applied Superconductivity*, 2019, vol. 29, no. 2, pp. 1-4. doi: <https://doi.org/10.1109/TASC.2019.2895677>.
17. Mosaad M.I., Abu-Siada A., El-Naggar M.F. Application of Superconductors to Improve the Performance of DFIG-Based WECS. *IEEE Access*, 2019, vol. 7, pp. 103760-103769. doi: <https://doi.org/10.1109/ACCESS.2019.2929261>.
18. Bizon N. Effective mitigation of the load pulses by controlling the battery/SMES hybrid energy storage system. *Applied Energy*, 2018, vol. 229, pp. 459-473. doi: <https://doi.org/10.1016/j.apenergy.2018.08.013>.
19. Qais M.H., Hasanien H.M., Alghuwainem S. Output power smoothing of wind power plants using self-tuned controlled SMES units. *Electric Power Systems Research*, 2020, vol. 178, art. no. 106056. doi: <https://doi.org/10.1016/j.epsr.2019.106056>.
20. Huang C., Zheng Z., Xiao X., Chen X. Cooperative strategy of SMES device and modified control for cost-effective fault ride-through enhancement and power smoothing of 10 MW class superconducting wind turbine. *Journal of Renewable and Sustainable Energy*, 2020, vol. 12, no. 3, art. no. 033302. doi: <https://doi.org/10.1063/1.5143565>.
21. Boudia A., Messalti S., Harrag A., Boukhnifer M. New hybrid photovoltaic system connected to superconducting magnetic energy storage controlled by PID-fuzzy controller. *Energy Conversion and Management*, 2021, vol. 244, art. no. 114435. doi: <https://doi.org/10.1016/j.enconman.2021.114435>.
22. Slootweg J.G., de Haan S.W.H., Polinder H., Kling W.L. General model for representing variable speed wind turbines in power system dynamics simulations. *IEEE Transactions on Power Systems*, 2003, vol. 18, no. 1, pp. 144-151. doi: <https://doi.org/10.1109/TPWRS.2002.807113>.
23. Soliman M.A., Hasanien H.M., Azazi H.Z., El-Kholy E.E., Mahmoud S.A. An Adaptive Fuzzy Logic Control Strategy for Performance Enhancement of a Grid-Connected PMSG-Based Wind Turbine. *IEEE Transactions on Industrial Informatics*, 2019, vol. 15, no. 6, pp. 3163-3173. doi: <https://doi.org/10.1109/TII.2018.2875922>.
24. Zine H.K.E., Abed K. Smart current control of the wind energy conversion system based permanent magnet synchronous generator using predictive and hysteresis model. *Electrical Engineering & Electromechanics*, 2024, no. 2, pp. 40-47. doi: <https://doi.org/10.20998/2074-272X.2024.2.06>.
25. Ali M.H., Park M., Yu I.-K., Murata T., Tamura J. Improvement of Wind-Generator Stability by Fuzzy-Logic-Controlled SMES. *IEEE Transactions on Industry Applications*, 2009, vol. 45, no. 3, pp. 1045-1051. doi: <https://doi.org/10.1109/TIA.2009.2018901>.
26. Zadeh L.A., Klir G.J., Yuan B. Fuzzy Sets, Fuzzy Logic, and Fuzzy Systems. *World Scientific*. 1996, vol. 6, 840 p. doi: <https://doi.org/10.1142/2895>.
27. Kaddache M., Drid S., Khemis A., Rahem D., Chrifi-Alaoui L. Maximum power point tracking improvement using type-2 fuzzy controller for wind system based on the double fed induction generator. *Electrical Engineering & Electromechanics*, 2024, no. 2, pp. 61-66. doi: <https://doi.org/10.20998/2074-272X.2024.2.09>.
28. Aissaoui M., Bouzeria H., Benidir M., Labeled M.A. Harmonics suppression in high-speed railway via single-phase traction converter with an LCL filter using fuzzy logic control strategy. *Electrical Engineering & Electromechanics*, 2024, no. 2, pp. 16-22. doi: <https://doi.org/10.20998/2074-272X.2024.2.03>.
29. Topaloglu F., Pehlivan H. Analysis of the effects of different fuzzy membership functions for wind power plant installation parameters. *2018 6th International Symposium on Digital Forensic and Security (ISDFS)*, 2018, pp. 1-6. doi: <https://doi.org/10.1109/ISDFS.2018.8355383>.
30. Aly M.M., Abdel-Akher M., Said S.M., Senjyu T. A developed control strategy for mitigating wind power generation transients using superconducting magnetic energy storage with reactive power support. *International Journal of Electrical Power & Energy Systems*, 2016, vol. 83, pp. 485-494. doi: <https://doi.org/10.1016/j.ijepes.2016.04.037>.
31. Mukherjee P., Rao V.V. Effective location of SMES for power fluctuation mitigation of grid connected doubly fed induction generator. *Journal of Energy Storage*, 2020, vol. 29, art. no. 101369. doi: <https://doi.org/10.1016/j.est.2020.101369>.

Received 17.09.2023
Accepted 18.03.2024
Published 20.08.2024

A. Nid¹, PhD Student,
S. Sayah¹, Professor,
A. Zebar¹, Doctor of Electrical Engineering,
¹Department of Electrical Engineering,
Farhat Abbas University, Setif, 19000, Algeria,
e-mail: abdelbasset.nid@univ-setif.dz (Corresponding Author);
samir.sayah@univ-setif.dz; abdelkrim.zebar@univ-setif.dz

How to cite this article:

Nid A., Sayah S., Zebar A. Power fluctuation suppression for grid connected permanent magnet synchronous generator type wind power generation system. *Electrical Engineering & Electromechanics*, 2024, no. 5, pp. 70-76. doi: <https://doi.org/10.20998/2074-272X.2024.5.10>